A new species of *Metopocetus* (Cetacea, Mysticeti, Cetotheriidae) from the Late Miocene of the Netherlands

Felix Georg Marx, Mark Bosselaers, Stephen Louwye

The family Cetotheriidae has played a major role in recent discussions of baleen whale phylogenetics. Within this group, the enigmatic, monotypic *Metopocetus durinasus* has been interpreted as transitional between herpetocetines and other members of the family, but so far has been restricted to a single, fragmentary skull of uncertain provenance and age. Here, we expand the genus and shed new light on its phylogenetic affinities and functional morphology by describing *Metopocetus hunteri* sp. nov. from the Late Miocene of the Netherlands. Unlike the holotype of *M. durinasus*, the material described here is confidently dated and preserves both the tympanic bulla and additional details of the basicranium. *M. hunteri* closely resembles *M. durinasus*, differing primarily in its somewhat less distally expanded compound posterior process of the tympanoperiotic. Both species are characterised by the development of an unusually large fossa on the ventral surface of the paroccipital process, which extends anteriorly on to the compound posterior process and completely floors the facial sulcus. In life, this enlarged fossa may have housed the posterior sinus and/or the articulation of the stylohyal, or else have given rise to an enlarged digastric muscle, as seen in the extant grey whale, *Eschrichtius robustus*.

A new species of *Metopocetus* (Cetacea, Mysticeti, Cetotheriidae) from the Late Miocene of the Netherlands

Felix G. Marx[1] Mark Bosselaers[2,3] and Stephen Louwye[4]

[1]Department of Geology and Palaeontology, National Museum of Nature and Science, 4-1-1 Amakubo, Tsukuba 305-0005, Japan. Corresponding author: felix.marx@otago.ac.nz.

[2]Directorate of Earth and History of Life, Royal Belgian Institute of Natural Sciences, Rue Vautier 29, 1000 Brussels, Belgium, mark.bosselaers@telenet.be.

[3]Zeeland Royal Society of Sciences, 4331 JE Middelburg, the Netherlands.

[4]Research Unit Palaeontology, Ghent University, Krijgslaan 281/S8, 9000 Ghent, Belgium, stephen.louwye@ugent.be.

Note to reviewers: illustrated cladistic scorings for the new material are available from MorphoBank, project 2225. They can be accessed for review purposes by visiting www.morphobank.org and entering the following on the login page:

e-mail address: 2225
password: Metopocetusreview

The data will be made publicly available as soon as soon as the paper is published.

Abstract: The family Cetotheriidae has played a major role in recent discussions of baleen whale phylogenetics. Within this group, the enigmatic, monotypic *Metopocetus durinasus* has been interpreted as transitional between herpetocetines and other members of the family, but so far has been restricted to a single, fragmentary skull of uncertain provenance and age. Here, we expand the genus and shed new light on its phylogenetic affinities and functional morphology by describing *Metopocetus hunteri* sp. nov. from the Late Miocene of the Netherlands. Unlike the holotype of *M. durinasus*, the material described here is confidently dated and preserves both the tympanic bulla and additional details of the basicranium. *M. hunteri* closely resembles *M. durinasus*, differing primarily in its somewhat less distally expanded compound posterior process of the tympanoperiotic. Both species are characterised by the development of an unusually large fossa on the ventral surface of the paroccipital process, which extends anteriorly on to the compound posterior process and completely floors the facial sulcus. In life, this enlarged fossa

may have housed the posterior sinus and/or the articulation of the stylohyal, or else have given rise to an enlarged digastric muscle, as seen in the extant grey whale, *Eschrichtius robustus*.

Keywords: Mysticeti, baleen whales, Metopocetus, Cetotheriidae, digastric, paroccipital concavity, phylogenetics, Late Miocene

Introduction

The Cetotheriidae play a crucial role in the evolution of baleen whales (Mysticeti). Long degraded to the state of a wastebasket taxon comprising nearly all fossil toothless mysticetes, the past decade saw the family restored to its original definition – *Cetotherium* and relatives – within a phylogenetic context (Bouetel & de Muizon 2006; Brandt 1873; Steeman 2007; Whitmore & Barnes 2008). The importance of this iconic family lies not only in its rather disparate morphology, which is clearly distinct from that of all living species and nearly survived until the present day (Boessenecker 2013), but also the still controversial idea that it may have given rise to the most enigmatic of the extant mysticetes, the pygmy right whale *Caperea marginata* (Fordyce & Marx 2013; Marx et al. 2013; Marx & Fordyce 2015). The phylogenetic position of the family relative to crown mysticetes remains a matter of debate, as does its exact composition and the interrelationships of the included species (Bisconti 2015; Bouetel & de Muizon 2006; Deméré et al. 2008; El Adli et al. 2014; Gol'din 2014; Gol'din & Startsev 2014; Kimura & Hasegawa 2010; Marx & Fordyce 2015; Steeman 2007).

There is wide agreement on the existence of at least one subfamily within the Cetotheriidae, comprising at least the closely related genera *Herpetocetus* and *Nannocetus* (Whitmore & Barnes 2008). The remaining cetotheriids are often partially or entirely lumped into the subfamily Cetotheriinae, although the definition of this grouping tends to vary across analysis (Bisconti 2015; El Adli et al. 2014; Gol'din & Startsev 2014; Marx & Fordyce 2015; Tarasenko & Lopatin 2012b). Within this context, the genus *Metopocetus* has been interpreted as a potentially intermediate form linking herpetocetines and cetotheriines (Whitmore & Barnes 2008); however, so far this taxon has had an unstable phylogenetic history (El Adli et al. 2014; Gol'din & Startsev 2014; Marx & Fordyce 2015; Steeman 2007).

At least in part, the uncertainty surrounding *Metopocetus* likely reflects the incomplete nature of the available material: to date, the genus has remained restricted to its type species, *M. durinasus*, which in turn is based on just a single, fragmentary skull (USNM 8518) missing the rostrum, tympanic bulla and much of the basicranium (Cope 1896; Kellogg 1968; Whitmore & Barnes 2008). The affinities of the only other putative occurrence of *Metopocetus*, "*M.*" *vandelli* from the Late Miocene of Portugal (Kellogg 1941), are doubtful (El Adli et al. 2014; Gol'din & Startsev 2014; Whitmore & Barnes 2008). Compounding things further are the lack of clear stratigraphic and provenance data for USNM 8518, which was collected from "a Miocene marl from near the mouth of the Potomac river" (Cope 1896: 143). Subsequent studies interpreted this statement to mean that the specimen was derived from either the Langhian portion of the Calvert Formation (Kellogg 1931; Kellogg 1968) or the Tortonian St. Mary's Formation (Case 1904).

Here, we describe a new species of *Metopocetus* from the Late Miocene of northwestern Europe (the Netherlands), the first material clearly representing this genus besides *M. durinasus*, and its first occurrence outside North America (Fig. 1). Unlike USNM 8518, the specimen described here is confidently dated and preserves both the tympanic bulla and additional details of the basicranium, thus providing new insights into cetothere phylogeny and functional morphology.

Material and methods

Morphological terminology follows Mead & Fordyce (2009), unless indicated. To determine the phylogenetic position of our new material, we added the specimen to the recently published matrix of Marx & Fordyce (2015: fig. 2) and repeated their dated total evidence analysis with all settings kept intact. The analysis was run in MrBayes 3.2.6, on the Cyberinfrastructure for Phylogenetic Research (CIPRES) Science Gateway (Miller et al. 2010). Our new morphological codings and the full matrix are available from MorphoBank, project 2225 (full matrix stored in the "Documents" section). To determine the age of the new specimen, we analysed a sample of the in situ sediment recovered from the skull for biostratigraphically informative palynomorphs. The extraction procedure followed the standard protocol of Louwye et al. (2007), and involved successive treatments with HCl and HF to remove carbonates and silicates, respectively. No

oxidation or ultrasonic treatment was applied to avoid damage and selective loss of species. The organic residue was mounted with glycerine jelly on two microscope slides, which were then systematically scanned for palynomorphs. Nomenclature of the dinoflagellate cysts follows Fensome et al. (2008).

The electronic version of this article in Portable Document Format (PDF) will represent a published work according to the International Commission on Zoological Nomenclature (ICZN), and hence the new names contained in the electronic version are effectively published under that Code from the electronic edition alone. This published work and the nomenclatural acts it contains have been registered in ZooBank, the online registration system for the ICZN. The ZooBank LSIDs (Life Science Identifiers) can be resolved and the associated information viewed through any standard web browser by appending the LSID to the prefix http://zoobank.org/. The LSID for this publication is: urn:lsid:zoobank.org:pub:E728C3DD-EB85-482F-ACE6-6558E3ED5441. The online version of this work is archived and available from the following digital repositories: PeerJ, PubMed Central and CLOCKSS.

Institutional abbreviations

MUHNAC, Museu Nacional de História Natural e da Ciência, Lisbon, Portugal; NMR, Natuurhistorisch Museum Rotterdam, the Netherlands; OU, Geology Museum, University of Otago, Dunedin, New Zealand; USNM, United States National Museum of Natural History, Washington DC, USA; ZMT, Fossil mammals catalogue, Canterbury Museum, Christchurch, New Zealand.

Biostratigraphy and environment

The preservation of the dinoflagellate cyst assemblage recovered from the sediment sample is moderate to good. In total, we recorded 28 dinoflagellate cyst species and three acritarchs (Supplementary Table 1), the most important of which include *Barssidinium taxandrianum*, *Gramocysta verricula*, *Habibacysta tectata*, *Hystrichosphaeropsis obscura* and *Labyrinthodinium truncatum*. *H. tectata* first occurs in the North Atlantic realm (Porcupine Basin, off southwest Ireland) during the Langhian, around 14.2 Ma (Hilgen et al. 2012; Louwye

et al. 2008; Quaijtaal et al. 2014), thus setting a maximum age for the sample. Conversely, the minimum age is determined by the highest occurrences of *Hy. obscura* and *L. truncatum* at approximately 7.6 Ma (de Verteuil & Norris 1996; Dybkjær & Piasecki 2010; Köthe 2012; Louwye & de Schepper 2010; Munsterman & Brinkhuis 2004).

The sample belongs to the late Tortonian SNSM14 Zone defined in the Netherlands (Munsterman & Brinkhuis 2004), which is equivalent to the *Hystrichosphaeropsis obscura* biozone of Denmark (Dybkjær & Piasecki 2010), and the DN9 Zone of the eastern USA and Germany (de Verteuil & Norris 1996; Köthe 2012), dated to ca 8.8–7.6 Ma (Dybkjær & Piasecki 2010). The upper boundary of the SNSM14 Zone is defined by the highest occurrence of *L. truncatum*, while the lower boundary is defined by highest occurrence of *Cleistosphaeridium placacanthum*, a distinctive dinoflagellate cyst species not recorded in our sample. Diagnostic species present in this zone are *G. verricula* and *Hy. obscura* (Munsterman & Brinkhuis 2004). Further evidence for this age assessment comes from the occurrence of *B. taxandrianum*, which is a rare species with a restricted occurrence in the Late Miocene of the southern North Sea Basin, including the Tortonian Diest and the latest Tortonian-Messinian Kasterlee Formations (Louwye 1999; Louwye & de Schepper 2010; Louwye et al. 2007; Louwye & Laga 2008). This species has never been recorded from Pliocene deposits.

Besides age determination, the recovered dinoflagellates also provide some insights into the depositional environment. In this context, the presence of *Gramocysta verricula* is particularly notable. This species was first recorded in Late Miocene deposits from the Gram well in Denmark, where it dominates the eponymous biozone (Piasecki 1980). The latter is furthermore characterised by the disappearance of neritic genera, such as *Achomosphaera* and *Tectatodinium*, and an overall reduction in the abundance of other dinocyst species. Together, these events likely reflect a marine regression, accompanied by high sedimentation rates and an enhanced influx of freshwater (Piasecki 1980). The preference of *G. verricula* for marginal marine environments is further corroborated by its occurrence in the shallow marine Kasterlee Formation and other deposits recording marked drops in sea level (Louwye et al. 2007).

Systematic palaeontology

Cetacea Brisson, 1762

Mysticeti Gray, 1864

Cetotheriidae Brandt, 1872

Metopocetus Cope, 1896

Type species. *Metopocetus durinasus* Cope, 1896

Emended diagnosis. Small to medium-sized cetotheriid differing from all other chaeomysticetes except cetotheriids in having a distally expanded compound posterior process of the tympanoperiotic bearing a floored facial sulcus, as well as medially convergent ascending processes of the maxillae bearing an enlarged, primary dorsal infraorbital foramen [new term]; further differs from all other chaeomysticetes except cetotheriids and balaenopterids in having the ascending process of the maxilla and the parietal overlap anteroposteriorly; and from balaenopterids in having the apex of the supraoccipital shield located posterior to the supraorbital process of the frontal. Differs from other cetotheriids, including neobalaenines, in lacking a well-developed lateral tuberosity of the periotic, and in having a better-defined mallear fossa and an extremely well-developed paroccipital concavity and tympanohyal; from all other cetotheres, except possibly *Joumocetus*, in having a distinctly triangular ascending process of the maxilla; from *Herpetocetus*, *Nannocetus*, *Cephalotropis* and neobalaenines in having the posterior portion of the zygomatic process of the squamosal offset from the lateral border of the exoccipital by a distinct angle; from *Herpetocetus*, *Nannocetus* and *Piscobalaena* in the presence of a squamosal cleft; from *Herpetocetus* and *Nannocetus* in having a smaller temporal exposure of the alisphenoid and in having a transversely oriented postglenoid process; from *Brandtocetus*, *Cetotherium*, *Joumocetus*, *Kurdalagonus*, "*Aulocetus*" *latus*, "*Cetotherium*" *megalophysum,* "*Metopocetus*" *vandelli* and likely also *Herentalia* in having a (slightly) more plug-like compound posterior process of the tympanoperiotic; from *Brandtocetus*, *Cephalotropis*, *Cetotherium*, *Joumocetus*, *Kurdalagonus*, *Vampalus*, *Zygiocetus*, "*Aulocetus*" *latus*, "*Cetotherium*" *megalophysum* and "*Metopocetus*" *vandelli* in having a more rounded apex of the supraoccipital shield; from *Brandtocetus*, *Cetotherium* and *Zygiocetus* in having a tympanic bulla that is not transversely wider anteriorly than it is posteriorly; and from *Joumocetus* and *Cephalotropis* in having the parietal almost excluded from the intertemporal region.

Metopocetus hunteri, sp. nov.

Figures 2–8

LSID. urn:lsid:zoobank.org:act:391CF6D9-138C-4F88-AC4B-9903DA433FDA

Holotype. NMR 9991-07729, a partial skull preserving the vertex, palatines, the right half of the braincase and basicranium, and the right periotic and tympanic bulla.

Locality and horizon. Sand pit at Liessel, Deurne, North Brabant, the Netherlands (Fig. 1). Breda Formation, Tortonian (Late Miocene), ca 8.8–7.6Ma (see discussion of biostratigraphy above).

Etymology. Named after the famous Scottish surgeon and anatomist John Hunter, who was maybe the first person to recognise and write about the similarity of whales and artiodactyls (Hunter 1787).

Diagnosis. Differs from *Metopocetus durinasus* in having a somewhat narrower, less distally exposed compound posterior process of the tympanoperiotic, a less anteriorly bulging temporal wall of the squamosal and a more proximally located primary dorsal infraorbital foramen on the ascending process of the maxilla (located either more distally or absent in *M. durinasus*), as well as in lacking ankylosed nasals.

Description

Overview. The preserved, mostly right portion of the skull lacks both the rostrum and the supraorbital process (Fig. 2). The apex of the zygomatic process, the central portion of the nuchal crest, the tip of the postglenoid process and much of the right pterygoid are broken. The state of preservation of the bones that remain is relatively good, but a certain degree of surface damage and small pockets of remaining matrix (e.g. on the dorsal surface of the periotic) sometimes make it difficult to discern details. Measurements of the skull are shown in Table 1.

Maxilla, premaxilla and nasal. Of the maxilla, only the triangular ascending process is preserved, which extends posteriorly beyond the base of the supraorbital process and overlaps

with the parietal (Figs 2, 3). Medially, the apices of the ascending processes are clearly convergent, but remain separated from each other by the well-developed nasals. Near the base of the ascending process, there is a large *primary dorsal infraorbital foramen* [new term] also found in other cetotheriids, which exits into a short, dorsomedially oriented sulcus (Fig. 3b). Anteromedial to this foramen, there are two elongate sulci without obvious foramina running parallel to the medial margin of the maxilla. Inside the narial fossa, the maxilla gives rise to a narrow shelf supporting the anterolateral corner of the nasal. Nothing remains of the premaxilla, but from the arrangement of the vertex it is clear that it did not extend as far posteriorly as the other rostral bones, and likely terminated somewhere along the anterior half of the nasal. In dorsal view, the nasal is anteroposteriorly elongate (Fig. 3b). Although transversely compressed posteriorly, it is exposed on the skull vertex along its entire length. The anterior portions of both nasals are eroded, but seem to have formed a straight or slightly convex anterior border, without any obvious sagittal crest.

Frontal. Only the portion of the frontal supporting the ascending process of the maxilla is preserved (Fig. 2). In dorsal view, the frontal is almost entirely excluded from the skull vertex by the maxilla, but still overrides much of the anterior portion of the parietal. Laterally, the posterior margin of the frontal gradually descends anteroventrally towards the base of the supraorbital process. In lateral view, the dorsal portion of the fronto-parietal suture is elevated into a ridge slightly overhanging the anteriormost portion of the parietal (Fig. 3a).

Parietal. In dorsal view, the parietal is exposed as a thin band on the vertex, anterior to the apex of the supraoccipital shield (Fig. 3b). Anteroventral to the vertex, the parietal becomes markedly concave as it descends towards the base of the supraorbital process of the frontal. In lateral view, the parietal is slightly longer anteroposteriorly than high dorsoventrally (Fig. 4a). The parieto-squamosal suture is smooth, with no obvious hint of a ridge-like eminence or a tubercle at the point where the suture meets the nuchal crest. There is no postparietal foramen (Fig. 3a).

Alisphenoid. The alisphenoid is exposed in the temporal fossa and contacts the parietal, the squamosal and the pterygoid. In lateral view, the preserved portion of the alisphenoid is nearly circular in outline and relatively large (Fig. 3a), though still much smaller than in *Herpetocetus* (El Adli et al. 2014). Anteroventrally, the alisphenoid likely contributed to the rim of the orbital fissure. In ventral view, the alisphenoid is covered by the dorsal lamina of the pterygoid.

Squamosal. In dorsal view, the temporal surface of the squamosal is relatively even and does not markedly bulge into the temporal fossa. The posterior border of the temporal fossa is smooth with no squamosal crease (Fig. 2a). There is a well-developed squamosal cleft that originates at the parieto-squamosal suture and runs towards the base of the zygomatic process (Fig. 3a). The squamosal fossa is anteroposteriorly elongate, with its floor being convex anteriorly, but concave posteriorly as it approaches the posterior apex of the nuchal crest. The zygomatic process is broken, but has a robust base bearing a distinct supramastoid crest and a small squamosal prominence (Fig. 2b). Judging from what remains, the zygomatic process seems to have been oriented anteriorly. Posteriorly, the zygomatic process is laterally offset from the rest of the skull, with its posterior border forming a 90 degree angle with the lateral margin of the exoccipital and the portion of the squamosal surrounding the periotic (Fig. 2a).

In lateral view, there is a well-defined sternomastoid fossa located just ventral to the supramastoid crest (Figs 2b, 4a). The preserved portion of the postglenoid process is triangular in outline and points slightly posteroventrally. The base of the zygomatic process is robust. In posterior view, the postglenoid is parabolic in outline and seems to point directly ventrally, although its exact shape it lost owing to breakage (Fig. 4b). The posterior meatal crest extends from the external acoustic meatus on to the posterior face of the postglenoid process, where it forms well-developed horizontal shelf. In doing so, it defines a deep sulcus running parallel to the meatus, immediately below the sternomastoid fossa (Figs 2b, 4b).

In ventral view, the falciform process of the squamosal is broad, distinctly squared and, along with adjacent portions of the squamosal, forms virtually the entire rim of the foramen pseudovale (Fig. 5). The external acoustic meatus is relatively broad, with its roof – the posterior meatal crest – extending on to the anterior face of the posterior process of the periotic. Together with the falciform process, the innermost portion of the internal acoustic meatus defines a strikingly rectangular window exposing the lateral surface of the anterior process of the periotic (Fig. 6a). Anterior to the meatus, the postglenoid process of the squamosal is thin anteroposteriorly, oriented transversely and medially confluent with the anterior meatal crest.

Supraoccipital. In dorsal view, the supraoccipital shield is broadly triangular, with a straight to slightly convex lateral border (= nuchal crest) and a rounded apex (Fig. 2a). The nuchal crest is oriented mostly dorsally and does not overhang the temporal fossa. Just posterior to the apex of

the supraoccipital shield, there is a relatively broad, tabular area that posteriorly gives rise to an external occipital crest. The latter is well-developed and extends along at least one third of the dorsal surface of the supraoccipital; further posteriorly, the central portion of the bone is missing (Fig. 2). In posterior view, the supraoccipital is markedly concave transversely, without any obvious tubercles on either side of the external occipital crest (Fig. 4b).

Exoccipital and basioccipital. In dorsal view, the exoccipital is well developed and extends posteriorly both beyond the level of the occipital condyle and the posterior apex of the nuchal crest (Fig. 2). The occipital condyle is large and situated on a short neck. In posterior view, the paroccipital process is squared in outline and extends ventrally to roughly the same level as the basioccipital crest (Fig. 4b). Medial to the paroccipital process, the jugular notch is narrow transversely and elongate dorsoventrally. The foramen magnum is large and framed by the dorsal portion of the occipital condyle.

In ventral view, the exoccipital is excavated by an extremely large paroccipital concavity (Fig. 6a). Medially, this fossa invades, and is thus partially floored by, the ventromedial corner of the paroccipital process, which also separates it from the jugular notch. Laterally, the paroccipital concavity is relatively open. Anteriorly, the floor of the paroccipital concavity forms a shelf that partially floors the facial sulcus, and is in turn underlapped by a *posteroventral flange* [new term] arising from the compound posterior process of the tympanoperiotic (Fig. 6a, c). This contact between the exoccipital and the posteroventral flange of the tympanoperiotic creates a continuous bony surface that allows the paroccipital concavity to extend far on to the tympanoperiotic itself (Figs 5, 6a, c). Medial to the well-marked jugular notch, the basioccipital crest is transversely broad, triangular and oriented anteroposteriorly (Fig. 5). As far as can be told, the suture between the basioccipital and the basisphenoid is ventrally covered by the posteriormost portion of the vomer.

Vomer. Only the posterior portion of the vomer is preserved. In the basicranium, the vomer is broadly exposed posterior to what remains of the choanae and overrides much of the medial lamina of the pterygoid. Further anteriorly, the vomer is exposed along the midline of the skull between the anterior portions of the palatines (Fig. 5).

Palatine. Both palatines are preserved, but have lost nearly all of their outer margins; they are markedly concave transversely as if "pinched", thus forming a distinct ventral keel.

Pterygoid. The ventral portion of the pterygoid is mostly missing, except for a small portion contributing to the rim of the foramen pseudovale. Dorsally, the pterygoid roofs almost the entire pterygoid sinus fossa, which extends anteriorly approximately to the level of the foramen pseudovale. Posteriorly, the dorsal or lateral lamina of the pterygoid overrides the anteriormost portion of the anterior process of the periotic (Figs 5, 6a). Medially, the pterygoid is continuous with the basioccipital crest.

Periotic, stapes and tympanohyal. In ventral view, the anterior process of the periotic appears to be transversely thickened, but not hypertrophied (Fig. 6a). The lateral tuberosity is indistinct. The anterior pedicle is relatively small and located just anterior to the broad and comparatively well-defined mallear fossa. There is no anterior bullar facet, and seemingly no distinct ridge for the attachment of the tensor tympani muscle. The pars cochlearis is rounded and posteriorly terminates in an elongate caudal tympanic process which approaches, but does not contact, the crista parotica (Fig. 6b). The presence or absence of a promontorial groove is unclear. Sediment obscures both the distal opening of the facial canal and the fenestra ovalis, but the ventral portion of the right stapes can be seen to protrude from the latter. The compound posterior process of the tympanoperiotic (hereafter "posterior process") is oriented posterolaterally relative to the anteroposterior axis of the pars cochlearis. At its base, it carries the posterior pedicle of the tympanic bulla, which appears curved as a result of internal excavation by the tympanic cavity (Fig. 6 a, b). Next to the posterior pedicle, there is an extremely large, trumpet-shaped tympanohyal fused to the crista parotica (Fig. 6b). Along its anterior margin, the posterior process gives rise to a posteriorly excavated *anteroventral flange* [new term], which anteriorly delimits the expanded paroccipital concavity (Fig. 6a, c). The floor of the paroccipital concavity is formed by a horizontal *posteroventral flange* [new term] that underlaps both the facial canal and the anterior rim of the ventral surface of the exoccipital (Fig. 6a, c).

In medial view, the anterior process appears two-bladed, but its actual shape is difficult to discern because it is partially covered by the dorsal/lateral lamina of the pterygoid. The fenestra rotunda is large and offset from the posterior border of the pars cochlearis by a broad shelf (Fig. 6b). Ventrally, this shelf merges with the elongate, posteriorly oriented caudal tympanic process.

In dorsal view, the internal acoustic meatus and the proximal opening of the facial canal are comparable in size and separated by a well-developed transverse septum (Fig. 6d). Together, they are nearly, albeit not perfectly, in line with the circular aperture for the cochlear aqueduct. The aperture for the vestibular aqueduct is obscured by matrix, but does not seem to overlap anterodorsally with the aperture for the cochlear aqueduct. The suprameatal fossa is shallow with a rounded lateral border; there is no distinct superior process. In lateral view, the posterior process is broadly exposed on the lateral skull wall, but anteroposteriorly narrower than in *Metopocetus durinasus* and herpetocetines (Fig. 6c) (Whitmore & Barnes 2008). The facial canal runs along the posterior border of the posterior process. Just anterior to the facial canal, there is a deep fossa of unknown function and homology, ventrally delimited by the expanded distal portion of the anteroventral flange (Fig. 6c).

Tympanic bulla. In dorsal view, the involucrum is relatively narrow in the area of the anteroposteriorly broad Eustachian outlet, but then rapidly widens as it approaches the posterior pedicle (Fig. 7a). There are no obvious transverse sulci on its dorsal surface, except for some poorly developed rims in the vicinity of the posterior pedicle. Transverse sulci are common in mysticetes and marked in adult specimens of at least some cetotheriids (e.g. *Brandtocetus chongulek* and *Herpetocetus transatlanticus*). It is possible that their absence in NMR 9991-07729 is a result of surface damage, although it seems likely that even in a perfectly preserved bulla they would have been at best faintly developed.

The involucral ridge extends all the way to the medial margin of the bulla, largely as a result of the robustness of the inner posterior prominence (= medial lobe of the tympanic bulla). The sigmoid process is oriented transversely and situated roughly halfway along the anteroposterior length of the bulla; its dorsomedial corner is distinct from the anterior process of the malleus and twisted slightly posteriorly. The conical process is located entirely posterior to the sigmoid process and is transversely thickened. Opposite the conical process, the posterior pedicle is located relatively close to the posterior border of the bulla and internally excavated by a branch of the tympanic cavity. In medial view, the bulla is somewhat pear-shaped in outline, with the dorsal surface of the involucrum being distinctly concave (Fig. 7b). In the region of the Eustachian outlet, the dorsal surface of the involucrum is depressed into abroad, smooth fossa. The main and involucral ridges converge anteriorly, while being more clearly separated

posteriorly by a relatively shallow median furrow and interprominential notch. On the medial face of the conical process, the tympanic sulcus follows a broad, horizontal ridge, before suddenly turning 90 degrees to run dorsally on to the posterior surface of the sigmoid process (Fig. 7g).

In ventral view, the anterior portion of the bulla appears to be more rounded than in most other cetotheriids, although the anterior border is still somewhat flattened (Fig. 7c). There is no anterolateral shelf. The anterolateral corner of the bulla is inflated and forms a distinct lobe anterior to the lateral furrow. The outline of the main ridge is convex. In lateral view, the lateral furrow is distinct and oriented vertically (Fig. 7d). The sigmoid cleft ventrally merges into the outer surface of the bulla, so that there is no discernable ventral border of the sigmoid process. Consequently, the latter does not overlap the anterior portion of the conical process, although the two processes are still connected by a well-developed horizontal rim. In anterior view, the ventral surface of the bulla is transversely convex, except for a small concave portion immediately medial to the main ridge (Fig. 7e). The rim of the Eustachian outlet is oriented horizontally and continuous with the dorsal surface of the involucrum. The lateral margin of the sigmoid process is oriented slightly dorsolaterally, but the process as a whole is not laterally deflected. In posterior view, the main ridge of the bulla is oriented medially, so that the inner posterior prominence faces dorsally, and the outer posterior prominence ventrally (Fig. 7f). Like most other chaeomysticetes, the bulla thus shows a marked degree of medial rotation relative to the condition in archaic toothed mysticetes and eomysticetids. The involucral ridge is well developed and terminates ventral to the base of the posterior pedicle. There is neither a transverse crest connecting the main and involucral ridges, nor an elliptical foramen. The lateral margin of conical process is straight.

Malleus. In posterodorsal view, the articular facets for the incus are oriented at right angles to each other, with the vertical facet being slightly larger (Fig. 8a). The head of the malleus is broadly rounded and separated from the tubercle by a distinct groove. In anterior view, the bottom of the head and the anterior process are excavated by the sulcus for the chorda tympani. Adjacent to the internal margin of the head, the muscular process bears a well-defined, circular pit for the insertion of the tendon of the tensor tympani muscle (Fig. 8b).

Discussion and conclusions

Phylogeny. The phylogenetic analysis clearly places *Metopocetus hunteri* inside both Cetotheriidae and the same genus as *M. durinasus* (Fig. 9). Beyond this, our results largely correspond to those of Marx and Fordyce (2015), but differ in three important aspects: (1) *Metopocetus* is no longer grouped with *Piscobalaena* and "*C.*" *megalophysum*, and instead now forms part of a basal lineage along with *Cephalotropis*; (2) *Piscobalaena* and "*C.*" *megalophysum* no longer cluster with the *Cetotherium* and instead are now sister to Herpetocetinae + Neobalaeninae; and (3) the Late Oligocene–Early Miocene clade including *Aglaocetus moreni*, *Mauicetus parki* and ZMT 67 is now basal to Cetotheriidae + Balaenopteroidea, instead of being included within balaenopteroids.

The grouping of *Metopocetus* and *Cephalotropis* is novel and somewhat surprising, given the superficially rather different morphologies of these taxa. Nevertheless, *Cephalotropis* has previously been found to occupy a basal position within Cetotheriidae (El Adli et al. 2014), which is at least partially reflected by our results. The move of *Piscobalaena* closer to herpetocetines is less controversial, and brings our findings into line with those of several earlier studies (Bisconti 2015; El Adli et al. 2014; Gol'din & Startsev 2014). Finally, the exclusion of *Aglaocetus moreni*, *Mauicetus parki* and ZMT 67 from Balaenopteroidea is the most fundamental of the three changes, but easily explained by the poor support for the position of these taxa both here and in the study of Marx and Fordyce (2015: fig. 2). All members of this clade remain only partially described and/or poorly known, and need to be studied further in comparison with a range of additional, equally enigmatic mysticete material of similar age and provenance (largely from New Zealand; e.g. Tsai & Fordyce 2015). Until more of these specimens are described and included in comprehensive phylogenetic analyses, the position of these archaic chaeomysticetes will likely continue to be unstable.

The relatively basal position of *Metopocetus* is inconsistent with it showing a morphology truly intermediate between that of herpetocetines and other cetotheriids (Whitmore & Barnes 2008). It furthermore implies that the pronounced widening of the distal portion of the compound posterior process – a hallmark of cetotheres – may have occurred more than once. The posterior process of *all* cetotheriids is large relative to that of most other mysticetes, but there are clear differences in scale: the posterior process is extremely expanded in herpetocetines,

neobalaenines, *Cephalotropis*, *M. durinasus* and *Piscobalaena*; somewhat less so in *Brandtocetus*, *Cetotherium*, *Kurdalagonus*, *M. hunteri* and *Zygiocetus*; and even less so in "*C.*" *megalophysum* and "*M.*" *vandelli*. Both of the latter were included in Herpetocetinae as sister to *Nannocetus* by El Adli et al. (2014), whereas "*C.*" *megalophysum* fell out as sister to *Piscobalaena* in the present analysis. Both topologies require that the distal widening of the posterior process either occurred in parallel in several lineages, or else was later reduced in certain species. There is, of course, a distinct possibility that this patchy character distribution is simply the result of errors in the cladistic hypotheses. Nevertheless, given the wide range of morphologies and generally mosaic distribution of characters within Cetotheriidae, we suggest that having an expanded posterior process may represent more of a shared evolutionary trend within the family, rather than a definitive uniting character. A better understanding of the history of this unique feature will likely depend on getting to grips with its function first.

Other records of *Metopocetus*. Besides *Metopocetus hunteri*, European rocks have yielded the remains of a wide range of other cetotheriids, including "*Aulocetus*" *latus*, *Cephalotropis* cf. *coronatus* and "*Metopocetus*" *vandelli* from Portugal (Kellogg 1941; Mocho & Póvoas 2010), *Herpetocetus* and *Herentalia* from Belgium (Bisconti 2015; Van Beneden 1882; Whitmore & Barnes 2008), "*Mesocetus*" *argillarius* from Denmark (Roth 1978), *Brandtocetus*, *Cetotherium*, *Kurdalagonus*, *Vampalus* and *Zygiocetus* from the region of the Eastern Paratethys (Brandt 1873; Gol'din 2014; Gol'din & Startsev 2014; Tarasenko 2014; Tarasenko & Lopatin 2012a; Tarasenko & Lopatin 2012b) and a variety of fragmentary and/or undescribed specimens recovered primarily from Belgium and the Netherlands (e.g. Bosselaers et al. 2004; Steeman 2010; Van Beneden 1886). Of these, "*Metopocetus*" *vandelli* (holotype: MUHNAC A1) is of particular interest to the present study, as it is the only other species ever referred to *Metopocetus* besides *M. durinasus* (Kellogg 1941). "*M.*" *vandelli* clearly differs from both *M. durinasus* and *M. hunteri* in a range of features, including (1) a more elongate, finger-like ascending process of the maxilla; (2) a more pointed, dorsally flattened supraoccipital shield lacking a well-developed external occipital crest; (3) the apparent absence of a squamosal cleft (not completely clear owing to incomplete preparation of the type specimen); (4) comparatively flat palatines not forming a medial ridge; and (5) a more gracile exoccipital (Fig. 10). In addition, the distal portion of the compound posterior process appears markedly less expanded in "*M.*" *vandelli*,

438 although the area surrounding the ear bones is damaged and its precise morphology therefore
439 difficult to discern.

440 Taken together, these differences speak against any particularly close affinity of "*M.*" *vandelli*
441 with *Metopocetus* and thus support its removal from this genus, as advocated by several other
442 recent studies (El Adli et al. 2014; Gol'din & Startsev 2014; Whitmore & Barnes 2008). One of
443 these studies suggested to transfer "*M.*" *vandelli* back to *Cetotherium* based on putative
444 morphological similarities (Whitmore & Barnes 2008), whereas the other two included this
445 species in a phylogenetic analysis and found it to be related either to "*Cetotherium*"
446 *megalophysum* (El Adli et al. 2014) or to a clade comprising *Piscobalaena*, *Metopocetus*,
447 *Nannocetus* and *Herpetocetus* (Gol'din & Startsev 2014).

448 With the sole exception of the apparent lack of a squamosal cleft, "*M.*" *vandelli* shares all of
449 the features that distinguish it for *Metopocetus* with "*C.*" *megalophysum*. Furthermore, an even
450 closer correspondence exists with "*Aulocetus*" *latus*, known from the same locality and horizon
451 (holotype MUNHAC A2): like "*M.*" *vandelli, "A." latus* seems to lack a squamosal cleft, and
452 both taxa have an even less developed external occipital crest than "*C.*" *megalophysum* (based on
453 USNM 10593 and 205510). In addition, "*M.*" *vandelli* and "*A.*" *latus* resemble each other in
454 having a distinctly sigmoidal dorsal portion of the parieto-squamosal suture, whereas the same
455 suture follows a simpler, anteriorly concave outline in "*C.*" *megalophysum*. We thus suggest that
456 "*M.*" *vandelli* and "*A.*" *latus* should be regarded as the same species, with the valid name being
457 "*M.*" *vandelli* Van Beneden, 1871. We furthermore concur with El Adli et al. (2014) that "*M.*"
458 *vandelli* and "*C.*" *megalophysum*, are closely related, and may form part of a single genus or
459 even the same species. The actual degree of difference will have to be established following a re-
460 preparation and more detailed study of the Portuguese material, to verify features such as the
461 seemingly absent squamosal cleft.

462 **Paroccipital concavity.** *Metopocetus* stands out for having an extremely enlarged paroccipital
463 concavity extending across both the exoccipital and the compound posterior process of the
464 tympanoperiotic (Fig. 6a). A fossa excavating the anteroventral surface of the paroccipital
465 process occurs in a variety of cetaceans, including archaeocetes, mysticetes and odontocetes (e.g.
466 Deméré & Berta 2008; Fraser & Purves 1960; Martínez Cáceres & de Muizon 2011). In
467 mysticetes, the fossa tends to be best developed in archaic forms and least in the extant taxa, but

its size and shape is variable (e.g. Deméré & Berta 2008; El Adli et al. 2014). The fossa is generally interpreted as the bony correlate of the posterior sinus and/or the site of the ligamentous attachment of the stylohyal to the basicranium (Beauregard 1894; Boessenecker & Fordyce 2014; Bouetel & de Muizon 2006; Deméré & Berta 2008; El Adli et al. 2014; Fraser & Purves 1960; Oelschläger 1986). Unfortunately, little has been published on either of these features in mysticetes, which makes it difficult to draw any firm conclusions.

Fraser and Purves (1960: plates 6 and 7) show the small posterior sinus of extant *Caperea marginata* and *Balaenoptera acutorostrata* as occupying only a fraction of what remains of the paroccipital concavity in these taxa. If correct, then this would imply that the sinus cannot by itself account for the development of the paroccipital concavity as a whole. However, it needs to be noted that their assessment was largely based on the interpretation of osteological correlates and a previous description of *B. acutorostrata* (without figures showing the posterior process) by Beauregard (1894), and hence may not be completely accurate. The ligamentous attachment of the stylohyal to the exoccipital in cetaceans has long been noted (Flower 1885), and an enlargement of this structure seems particularly plausible in the case of *Metopocetus* with its well-developed tympanohyal. Nevertheless, it remains questionable whether the ligament would have filled the entire space defined by the paroccipital concavity.

Another factor that may contribute to the development of the concavity became clear during a recent dissection of a juvenile grey whale, *Eschrichtius robustus*. In this species, the ventral surface of the exoccipital gives rise to an enlarged digastric muscle, which is responsible for lower jaw abduction (El Adli & Deméré 2015). The paroccipital concavity of *E. robustus* is larger and better-defined than in any other living mysticete, and, along with an enlarged angular process of the mandible on to which the digastric inserts, occurs in both juvenile and adult individuals (Fig. 11). In this light, it is tempting to speculate that, at least in baleen whales, the size of the paroccipital concavity may be a general indicator for the development of the digastric. If so, then this muscle was likely even larger in *Metopocetus* than in *Eschrichtius*, corroborating previous studies that inferred the presence of a sizeable digastric in other cetotheriids based on the widespread enlargement of the angular process of the mandible in this family (El Adli et al. 2014; Gol'din 2014).

El Adli and Deméré (2015) suggested that the larger digastric of *E. robustus* relative to rorquals might reflect a greater importance of muscular abduction, since grey whales cannot rely on the kinetic energy of a forward lunge to help drive down the mandibles (Arnold et al. 2005; Lambertsen et al. 1995; Orton & Brodie 1987). This explanation is plausible, but cannot easily account for the yet better-developed digastric of *Metopocetus* and other cetotheriids. Recent discussions of cetotheriid feeding strategies have focussed on the possibility of suction feeding, given that these whales seem poorly equipped for both rorqual-like lunge feeding, owing their often narrow rostrum and restricted gape, and balaenid-like skim feeding, owing to their usually flattened rostrum and thus presumably short baleen (El Adli et al. 2014; Gol'din 2014). In terms of their well-developed angular process, short baleen and, at least in some taxa, seemingly enhanced ability to rotate the mandible along its longitudinal axis (El Adli et al. 2014), cetotheriids most closely resemble *E. robustus*, which is known to be a benthic suction feeder (Ray & Schevill 1974; Werth 2000). Exactly how an enlarged digastric might function in this context is unclear, especially considering that in *E. robustus* opening the mouth for feeding seems to be achieved mainly via outwards rotation of the lips, rather than the lowering of the mandible (Ray & Schevill 1974). More research into the poorly known anatomy of the digastric in living mysticetes, as well as its attachment and size in other cetotheriids, may help to clarify this issue.

Acknowledgements

We thank Klaas Post for donating the specimen and allowing us to study it; XX for their comments on the manuscript; R. Ewan Fordyce for insightful discussions and providing the photograph of *Metopocetus durinasus*; Seraina Klopfstein for technical advice on the total evidence analysis; Carl Buell for providing illustrative drawings of living and fossil cetaceans; and the staff of all of the institutions involved for access to material and help during our visits.

Additional Information and Declarations

Funding

FGM was supported by a Japan Society for the Promotion of Science Postdoctoral Fellowship for Foreign Researchers.

Competing interests

There are no competing interests.

Author contributions

FGM described the material and performed the phylogenetic analysis. MB prepared the specimen and contributed to its description. SL carried out the palynological analysis. All authors contributed to the design of the study, discussed age assessments and character definitions, and wrote the paper.

References

Arnold PW, Birtles RA, Sobtzick S, Matthews M, and Dunstan A. 2005. Gulping behaviour in rorqual whales: underwater observations and functional interpretation. *Memoirs of the Queensland Museum* 51:309-332.

Beauregard H. 1894. Recherches sur l'appareil auditif chez les mammifères III. *Journal de l'Anatomie et de la Physiologie* 30:366-413.

Bisconti M. 2015. Anatomy of a new cetotheriid genus and species from the Miocene of Herentals, Belgium, and the phylogenetic and palaeobiogeographical relationships of Cetotheriidae s.s. (Mammalia, Cetacea, Mysticeti). *Journal of Systematic Palaeontology* 13:377-395.

Boessenecker RW. 2013. Pleistocene survival of an archaic dwarf baleen whale (Mysticeti: Cetotheriidae). *Naturwissenschaften* 100:365-371.

Boessenecker RW, and Fordyce RE. 2014. A new eomysticetid (Mammalia: Cetacea) from the Late Oligocene of New Zealand and a re-evaluation of '*Mauicetus*' *waitakiensis*. *Papers in Palaeontology*:published online.

Bosselaers M, Herman J, Hoedemakers K, Lambert O, Marquet R, and Wouters K. 2004. Geology and palaeontology of a temporary exposure of the Late Miocene Deurne Sand Member in Antwerpen (N. Belgium). *Geologica Belgica* 7:27-39.

Bouetel V, and de Muizon C. 2006. The anatomy and relationships of *Piscobalaena nana* (Cetacea, Mysticeti), a Cetotheriidae s.s. from the early Pliocene of Peru. *Geodiversitas* 28:319-395.

554 Brandt JF. 1873. Untersuchungen über die fossilen und subfossilen Cetaceen Europa's. *Mémoires de*
555 *l'Académie impériale des sciences de St-Pétersbourg* 20:1-371.
556 Case EC. 1904. Mammalia. In: Clark WB, ed. *Miocene*. Baltimore: The John Hopkins Press, 3-57.
557 Cope ED. 1896. Sixth contribution to the knowledge of the Miocene fauna of North Carolina.
558 *Proceedings of the American Philosophical Society* 35:139–146.
559 de Verteuil L, and Norris G. 1996. Miocene dinoflagellate stratigraphy and systematics of Maryland and
560 Virginia. *Micropaleontology* 42 (Suppl.):1-172.
561 Deméré TA, and Berta A. 2008. Skull anatomy of the Oligocene toothed mysticete *Aetioceus weltoni*
562 (Mammalia; Cetacea): Implications for mysticete evolution and functional anatomy. *Zoological*
563 *Journal of the Linnean Society* 154:308-352.
564 Deméré TA, McGowen MR, Berta A, and Gatesy J. 2008. Morphological and molecular evidence for a
565 stepwise evolutionary transition from teeth to baleen in mysticete whales. *Systematic Biology*
566 57:15-37.
567 Dybkjær K, and Piasecki S. 2010. Neogene dinocyst zonation for the eastern North Sea Basin, Denmark.
568 *Review of Palaeobotany and Palynology* 161:1-29.
569 El Adli JJ, and Deméré TA. 2015. On the anatomy of the temporomandibular joint and the muscles that
570 act upon it: observations on the gray whale, *Eschrichtius robustus*. *The Anatomical Record*
571 298:680-690.
572 El Adli JJ, Deméré TA, and Boessenecker RW. 2014. *Herpetocetus morrowi* (Cetacea: Mysticeti), a new
573 species of diminutive baleen whale from the Upper Pliocene (Piacenzian) of California, USA,
574 with observations on the evolution and relationships of the Cetotheriidae. *Zoological Journal of*
575 *the Linnean Society* 170:400-466.
576 Fensome RA, MacRae RA, and Williams GL. 2008. DINOFLAJ2, Version 1. Data Series no 1: American
577 Association of Stratigraphic Palynologists. p 937.
578 Flower WH. 1885. *An Introduction to the Osteology of the Mammalia*. London: Macmillan and Co.
579 Fordyce RE, and Marx FG. 2013. The pygmy right whale *Caperea marginata*: the last of the cetotheres.
580 *Proceedings of the Royal Society B* 280:20122645.
581 Fraser FC, and Purves PE. 1960. Hearing in cetaceans. *Bulletin of the British Museum (Natural History)*
582 *Zoology* 7:3-139.
583 Gol'din P. 2014. The anatomy of the Late Miocene baleen whale *Cetotherium riabinini* from Ukraine.
584 *Acta Palaeontologica Polonica* 59:795-814.
585 Gol'din P, and Startsev D. 2014. *Brandtocetus*, a new genus of baleen whales (Cetacea, Cetotheriidae)
586 from the Late Miocene of Crimea, Ukraine. *Journal of Vertebrate Paleontology* 34:419-433.

587 Hilgen FJ, Lourens LJ, and Van Dam JA. 2012. The Neogene Period. In: Gradstein FM, Ogg JG, Schmitz
588 M, and Ogg G, eds. *The Geologic Time Scale 2012*. Oxford: Elsevier, 923–978.
589 Hunter J. 1787. Observations on the structure and oeconomy of whales. *Philosophical Transactions of the*
590 *Royal Society of London B* 77:371-450.
591 Kellogg R. 1931. Pelagic mammals of the Temblor Formation of the Kern River region, California.
592 *Proceedings of the California Academy of Sciences* 19:217-397.
593 Kellogg R. 1941. On the cetotheres figured by Vandelli. *Boletim do Museu e Laboratório Mineralógico e*
594 *Geológico da Faculdade de Ciências da Universidade de Lisboa* 7-8:13-23.
595 Kellogg R. 1968. Fossil marine mammals from the Miocene Calvert Formation of Maryland and Virginia,
596 part 5: Miocene Calvert mysticetes described by Cope. *United States National Museum Bulletin*
597 247:103-132.
598 Kimura T, and Hasegawa Y. 2010. A new baleen whale (Mysticeti: Cetotheriidae) from the earliest late
599 Miocene of Japan and a reconsideration of the phylogeny of cetotheres. *Journal of Vertebrate*
600 *Paleontology* 30:577-591.
601 Köthe A. 2012. A revised Cenozoic dinoflagellate cyst and calcareous nannoplankton zonation for the
602 German sector of the southeastern North Sea Basin. *Newsletters on Stratigraphy* 45:189-220.
603 Lambertsen R, Ulrich N, and Straley J. 1995. Frontomandibular stay of Balaenopteridae: a mechanism for
604 momentum recapture during feeding. *Journal of Mammalogy* 76:877-899.
605 Louwye S. 1999. New species of organic-walled dinoflagellates and acritarchs from the Upper Miocene
606 Diest Formation, northern Belgium (southern North Sea Basin). *Review of Palaeobotany and*
607 *Palynology* 107:109-123.
608 Louwye S, and de Schepper S. 2010. The Miocene–Pliocene hiatus in the southern North Sea Basin
609 (northern Belgium) revealed by dinoflagellate cysts. *Geological Magazine* 147:760-776.
610 Louwye S, de Schepper S, Laga P, and Vandenberghe N. 2007. The Upper Miocene of the southern North
611 Sea Basin (northern Belgium): a palaeoenvironmental and stratigraphical reconstruction using
612 dinoflagellate cysts. *Geological Magazine* 144:33-52.
613 Louwye S, Foubert A, Mertens K, and van Rooij D. 2008. Integrated stratigraphy and palaeoecology of
614 the Lower and Middle Miocene of the Porcupine Basin. *Geological Magazine* 145:321-344.
615 Louwye S, and Laga P. 2008. Dinoflagellate cyst stratigraphy and palaeoenvironment of the marginal
616 marine Middle and Upper Miocene of the eastern Campine area, northern Belgium (southern
617 North Sea Basin). *Geological Journal* 43:75-94.
618 Martínez Cáceres M, and de Muizon C. 2011. A new basilosaurid (Cetacea, Pelagiceti) from the Late
619 Eocene to Early Oligocene Otuma Formation of Peru. *Comptes Rendus Palevol* 10:517-526.

Marx F, Buono M, Fordyce RE, and Boessenecker RW. 2013. Juvenile morphology: a clue to the origins of the most mysterious of mysticetes? *Naturwissenschaften* 100:257-261.

Marx FG, and Fordyce RE. 2015. Baleen boom and bust: a synthesis of mysticete phylogeny, diversity and disparity. *Royal Society Open Science* 2:140434.

Mead JG, and Fordyce RE. 2009. The therian skull: a lexicon with emphasis on the odontocetes. *Smithsonian Contributions to Zoology* 627:1-248.

Miller MA, Pfeiffer W, and Schwartz T. 2010. Creating the CIPRES Science Gateway for inference of large phylogenetic trees. Proceedings of the Gateway Computing Environments Workshop (GCE), 14 Nov 2010. New Orleans. p 1-8.

Mocho P, and Póvoas L. 2010. Contribucao para revisao sistematica de um cranio de *Cephalotropis* Cope, 1896 (Cetacea: Cetotheriidae) do Miocenico superior (Tortoniano inferior) da Adica (Sesimbra, Portugal). *Publicaciones del Seminario de Paleontología de Zaragoza* 9:180-183.

Munsterman DK, and Brinkhuis H. 2004. A southern North Sea Miocene dinoflagellate cyst zonation. *Geologie en Mijnbouw* 83:267-285.

Oelschläger HA. 1986. Comparative morphology and evolution of the otic region in toothed whales (Cetacea, Mammalia). *American Journal of Anatomy* 177:353-368.

Orton LS, and Brodie PF. 1987. Engulfing mechanics of fin whales. *Canadian Journal of Zoology* 65:2898-2907.

Piasecki S. 1980. Dinoflagellate cyst stratigraphy of the Miocene Hodde and Gram formations, Denmark. *Bulletin of the Geological Society of Denmark* 29:53-76.

Quaijtaal W, Donders TH, Persico D, and Louwye S. 2014. Characterising the middle Miocene Mi-events in the Eastern North Atlantic realm: A first high-resolution marine palynological record from the Porcupine Basin. *Palaeogeography, Palaeoclimatology, Palaeoecology* 399:140-159.

Ray GC, and Schevill WE. 1974. Feeding of a captive gray whale *Eschrichtius robustus*. *Marine Fisheries Review* 36:31-38.

Roth F. 1978. *Mesocetus argillarius* sp.n. (Cetacea, Mysticeti) from Upper Miocene of Denmark, with remarks on the lower jaw and the echolocation system in whale phylogeny. *Zoologica Scripta* 7:63-79.

Steeman EM. 2007. Cladistic analysis and a revised classification of fossil and recent mysticetes. *Zoological Journal of the Linnean Society* 150:875-894.

Steeman ME. 2010. The extinct baleen whale fauna from the Miocene-Pliocene of Belgium and the diagnostic cetacean ear bones. *Journal of Systematic Palaeontology* 8:63-80.

652 Tarasenko KK. 2014. New genera of baleen whales (Cetacea, Mammalia) from the Miocene of the
653 northern Caucasus and Ciscaucasia: 3. *Zygiocetus* gen. nov. (Middle Sarmatian, Adygea).
654 *Paleontological Journal* 48:551-562.
655 Tarasenko KK, and Lopatin AV. 2012a. New baleen whale genera (Cetacea, Mammalia) from the
656 Miocene of the northern Caucasus and Ciscaucasia: 1. *Kurdalagonus* gen. nov. from the middle-
657 late Sarmatian of Adygea. *Paleontological Journal* 46:531-542.
658 Tarasenko KK, and Lopatin AV. 2012b. New baleen whale genera (Cetacea, Mammalia) from the
659 Miocene of the northern Caucasus and Ciscaucasia: 2. *Vampalus* gen. nov. from the Middle-Late
660 Miocene of Chechnya and Krasnodar Region. *Paleontological Journal* 46:620-629.
661 Tsai C-H, and Fordyce RE. 2015. The earliest gulp-feeding mysticete (Cetacea: Mysticeti) from the
662 Oligocene of New Zealand. *Journal of Mammalian Evolution*:published online.
663 Van Beneden P-J. 1882. Description des ossements fossiles des environs d'Anvers. Troisième partie.
664 Cétacés. Genres *Megaptera*, *Balaenoptera*, *Burtinopsis* et *Erpetocetus*. *Annales du Musée Royal*
665 *d'Histoire Naturelle de Belgique* 7:1-87.
666 Van Beneden P-J. 1886. Description des ossements fossiles des environs d'Anvers. Cinquième partie.
667 Cétacés. Genres *Amphicetus*, *Heterocetus*, *Mesocetus*, *Idiocetus* et *Isocetus*. *Annales du Musée*
668 *Royal d'Histoire Naturelle de Belgique* 13:1-139.
669 Werth AJ. 2000. Feeding in marine mammals. In: Schwenk K, ed. *Feeding: Form, Function and*
670 *Evolution in Tetrapods*. San Diego: Academic Press, 487-526.
671 Whitmore FC, Jr, and Barnes LG. 2008. The Herpetocetinae, a new subfamily of extinct baleen whales
672 (Mammalia, Cetacea, Cetotheriidae). *Virginia Museum of Natural History Special Publication*
673 14:141-180.

674

675 **Figure captions**

676 **Figure 1.** Type locality of *Metopocetus hunteri*. Drawing of cetotheriid by Carl Buell.

677 **Figure 2.** Cranium of *Metopocetus hunteri* in (a) dorsal and (b) posterolateral view.

678 **Figure 3.** Detail of the cranium of *Metopocetus hunteri*: (a) posteromedial wall of temporal fossa
679 in anteromedial view; (b) vertex in anterodorsal view.

680 **Figure 4.** Cranium of *Metopocetus hunteri* in (a) lateral and (b) posterior view.

Figure 5. Cranium of *Metopocetus hunteri* in ventral view.

Figure 6. Basicranium and periotic of *Metopocetus hunteri*: (a) right portion of basicranium in ventral view; (b) central portion of periotic in ventromedial view; (c) compound posterior process of tympanoperiotic in external view; (d) central portion of periotic in dorsal view. Abbreviations: fac., facial sulcus; parocc. conc., paroccipital concavity; post. process, compound posterior process.

Figure 7. Tympanic bulla of *Metopocetus hunteri* in (a) dorsal, (b) medial, (c) ventral, (d) lateral, (e) anterior, (f) posterior and (g) slightly oblique dorsomedial view.

Figure 8. Malleus of *Metopocetus hunteri* in (a) posterior and (b) anterior view.

Figure 9. Phylogenetic relationships of *Metopocetus hunteri*, based on a dated total evidence analysis. All data except the codings for *M. hunteri* are from Marx & Fordyce (2015: fig. 2). Drawings of cetaceans by Carl Buell.

Figure 10. Morphological features distinguishing "*Metopocetus*" *vandelli* from *M. durinasus* and *M. hunteri*. Skulls in dorsal view.

Figure 11. Left portion of the basicranium of the extant grey whale, *Eschrichtius robustus*, in ventrolateral view, highlighting the position of the paroccipital concavity.

704

Figure 1(on next page)

Type locality of *Metopocetus hunteri*

Figure 1. Type locality of *Metopocetus hunteri*. Drawing of cetotheriid by Carl Buell.

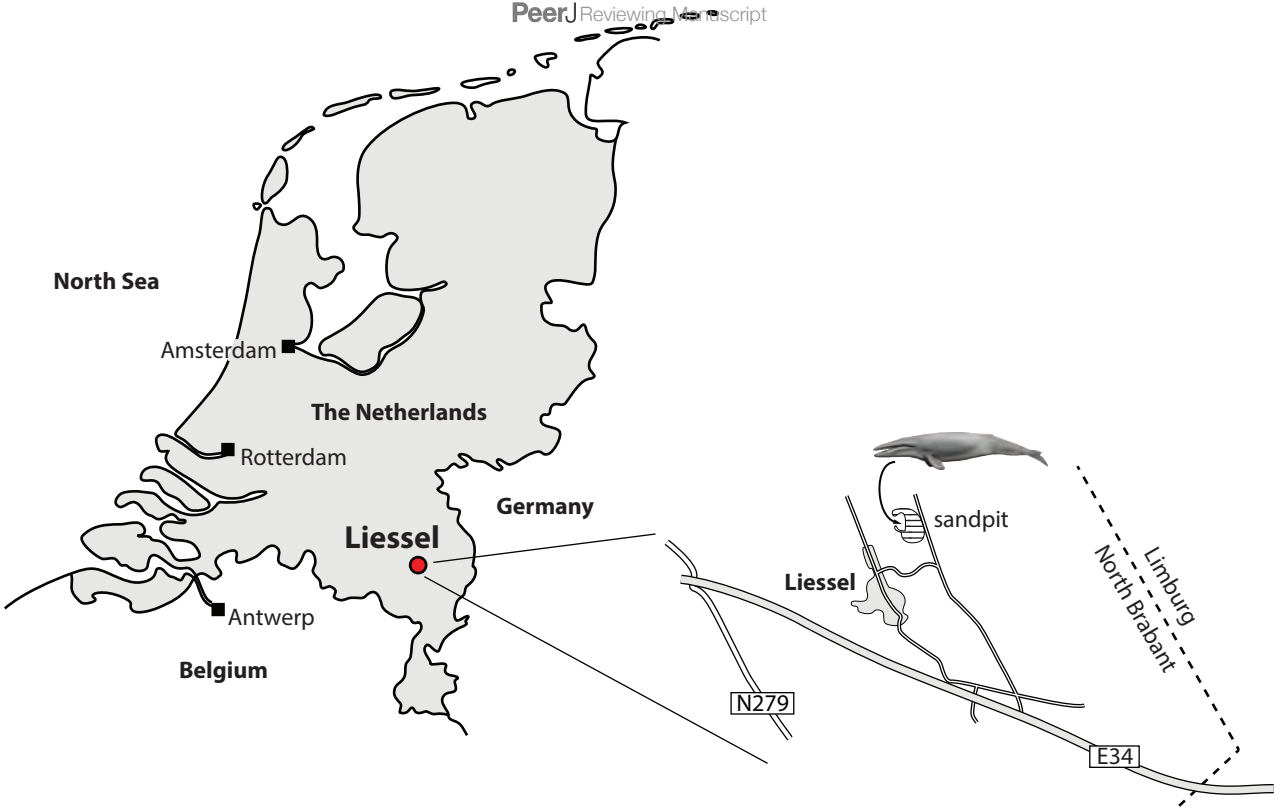
North Sea
Amsterdam
The Netherlands
Rotterdam
Germany
Liessel
Antwerp
Belgium
sandpit
Liessel
Limburg
North Brabant
N279
E34

Figure 2(on next page)

Cranium in dorsal view

Figure 2. Cranium of *Metopocetus hunteri* in (a) dorsal and (b) posterolateral view.

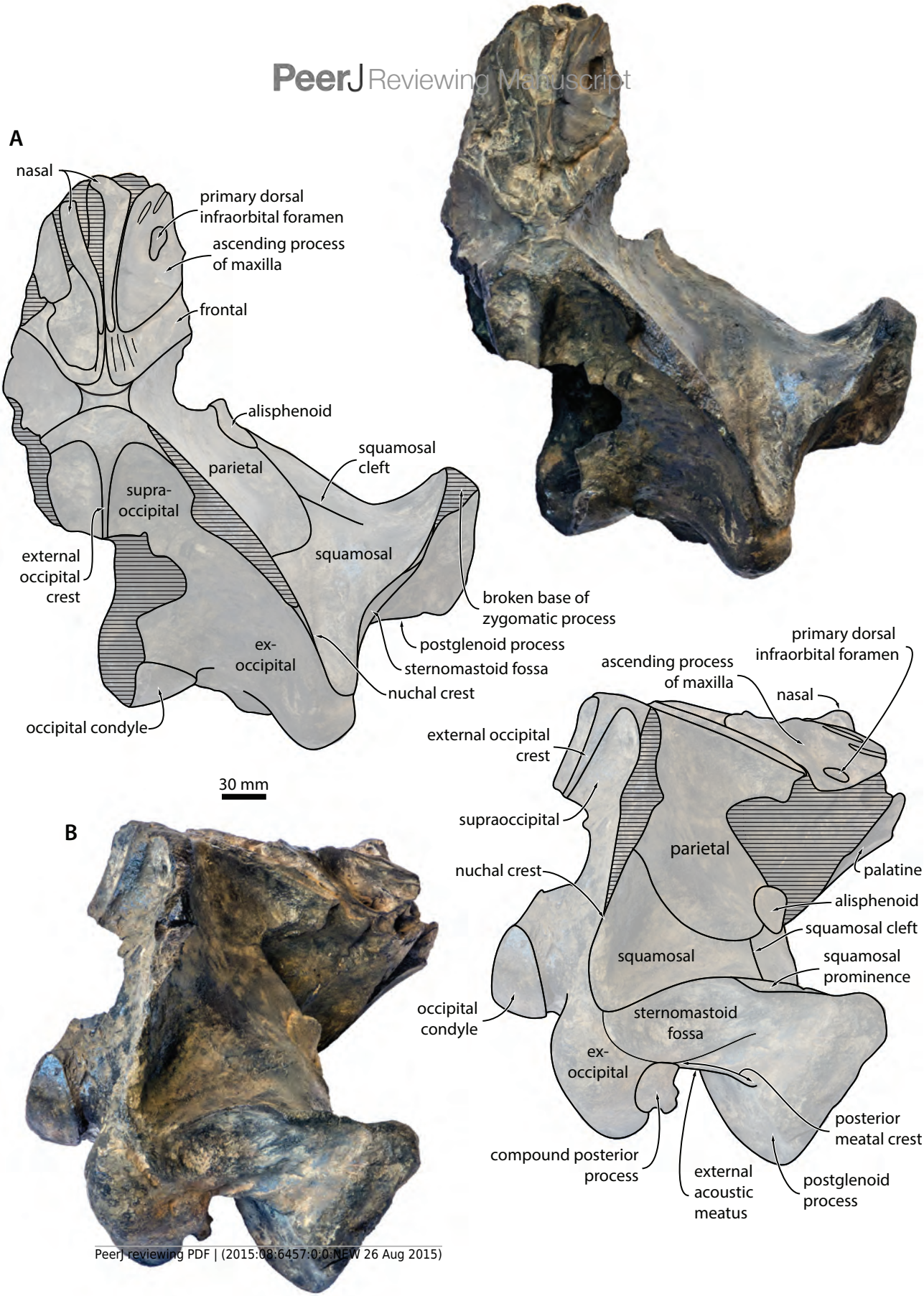

Figure 3(on next page)

Temporal fossa and vertex

Figure 3. Detail of the cranium of *Metopocetus hunteri*: (a) posteromedial wall of temporal fossa in anteromedial view; (b) vertex in anterodorsal view.

A

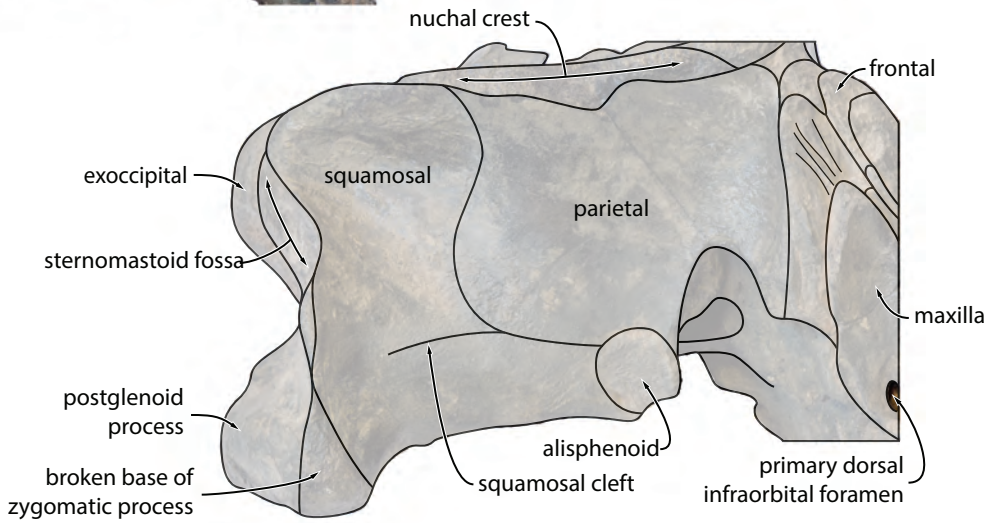

B

30 mm

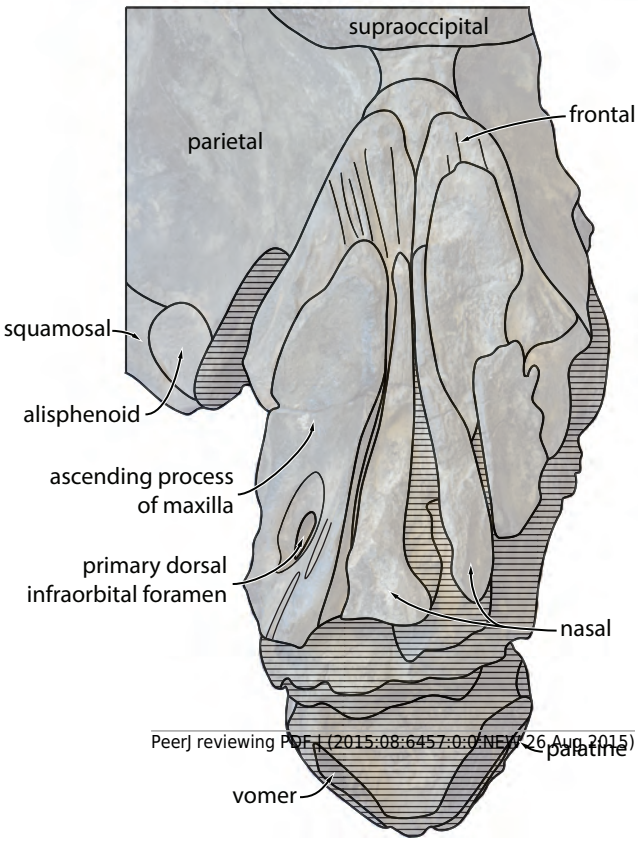

Figure 4(on next page)

Cranium in lateral and posterior view

A

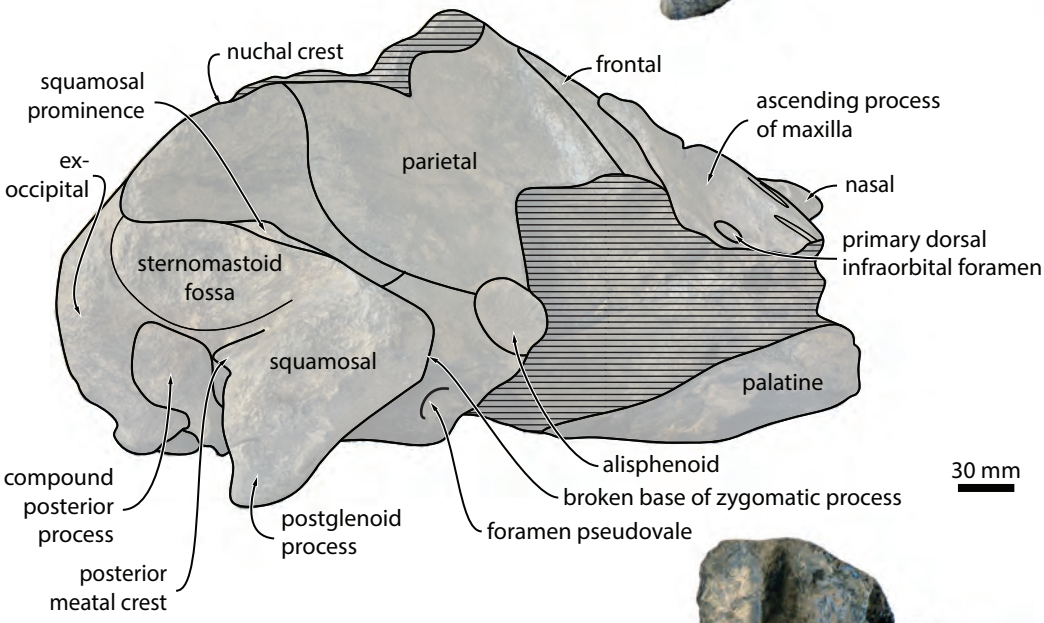

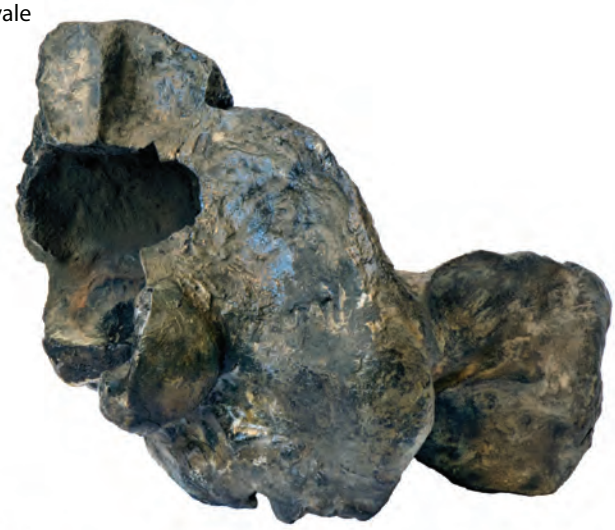

B

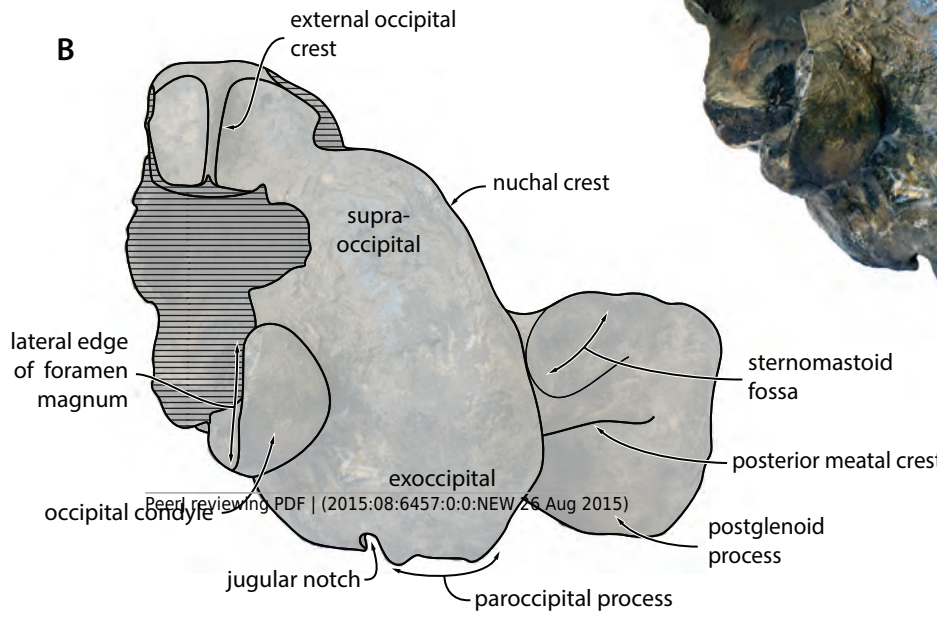

Figure 5(on next page)

Cranium in ventral view

Figure 5. Cranium of *Metopocetus hunteri* in ventral view.

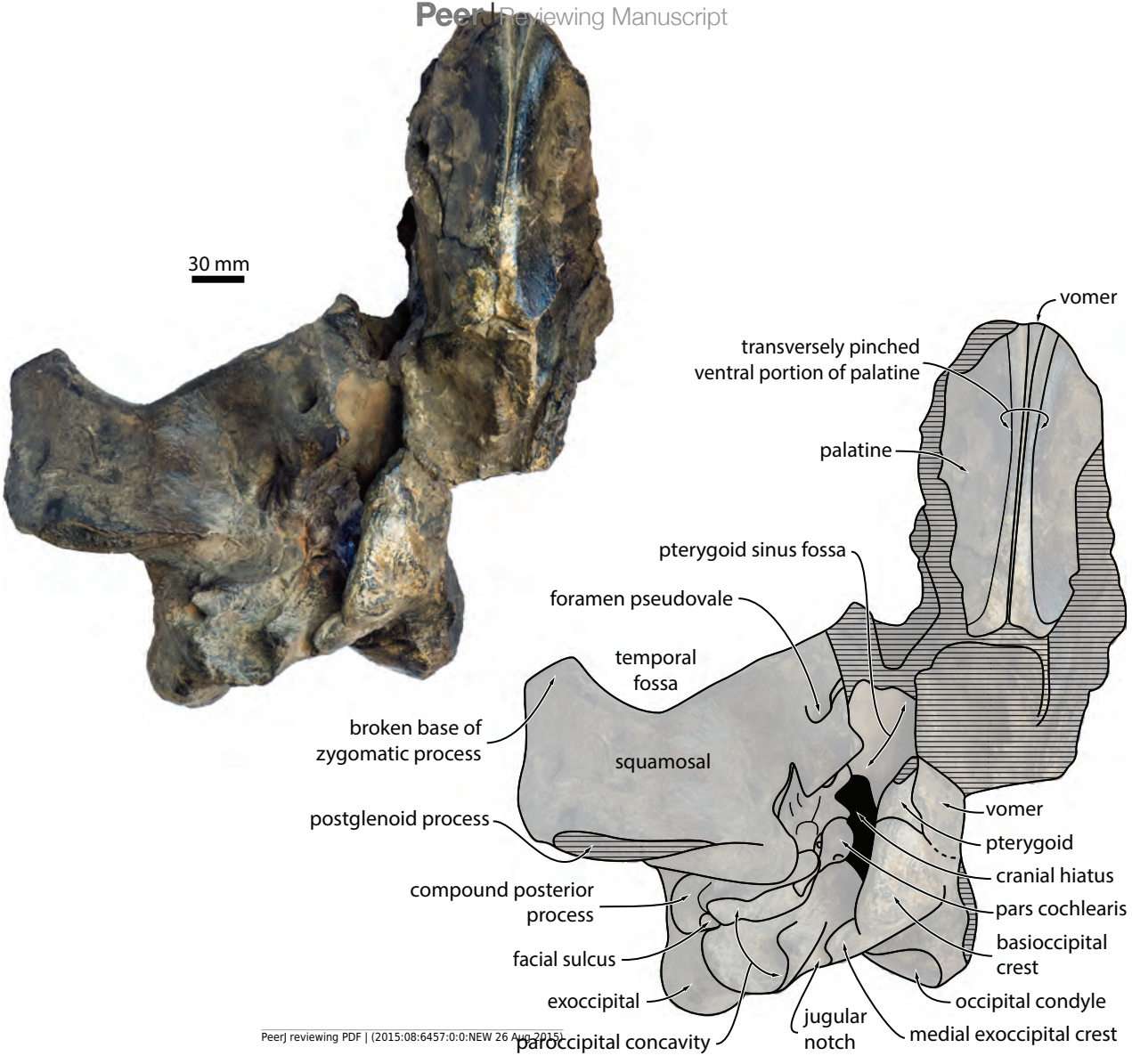
30 mm
vomer
transversely pinched ventral portion of palatine
palatine
pterygoid sinus fossa
foramen pseudovale
temporal fossa
broken base of zygomatic process
squamosal
postglenoid process
vomer
pterygoid
cranial hiatus
compound posterior process
pars cochlearis
basioccipital crest
facial sulcus
exoccipital
occipital condyle
jugular notch
medial exoccipital crest
paroccipital concavity

Figure 6(on next page)

Basicranium and periotic

Figure 6. Basicranium and periotic of *Metopocetus hunteri*: (a) right portion of basicranium in ventral view; (b) central portion of periotic in ventromedial view; (c) compound posterior process of tympanoperiotic in external view; (d) central portion of periotic in dorsal view. Abbreviations: fac., facial sulcus; parocc. conc., paroccipital concavity; post. process, compound posterior process.

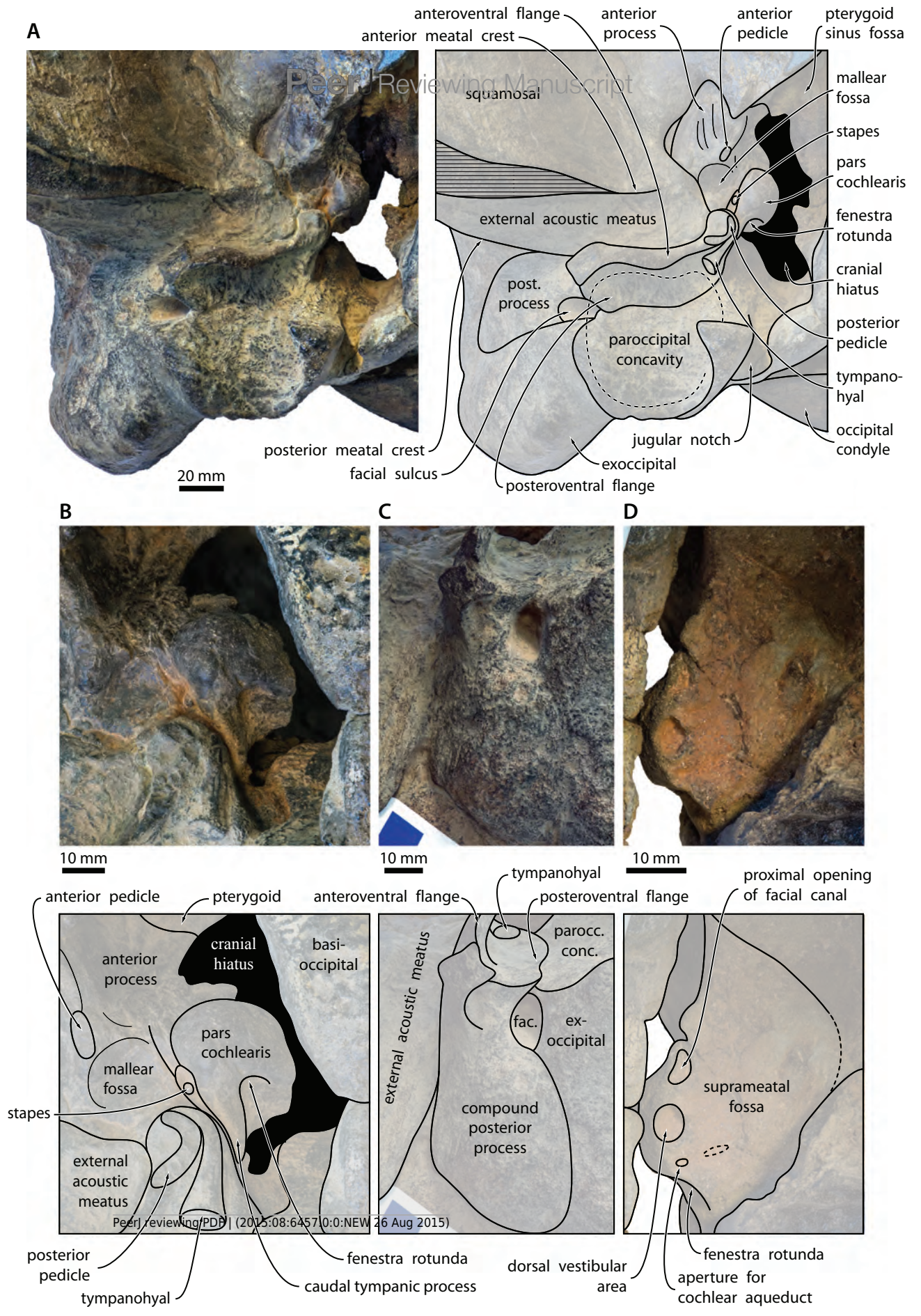

Figure 7(on next page)

Tympanic bulla - photographs

Figure 7. Tympanic bulla of *Metopocetus hunteri* in (a) dorsal, (b) medial, (c) ventral, (d) lateral, (e) anterior, (f) posterior and (g) slightly oblique dorsomedial view.

Figure 8(on next page)

Tympanic bulla - explanatory line drawings

Figure 7 - continued

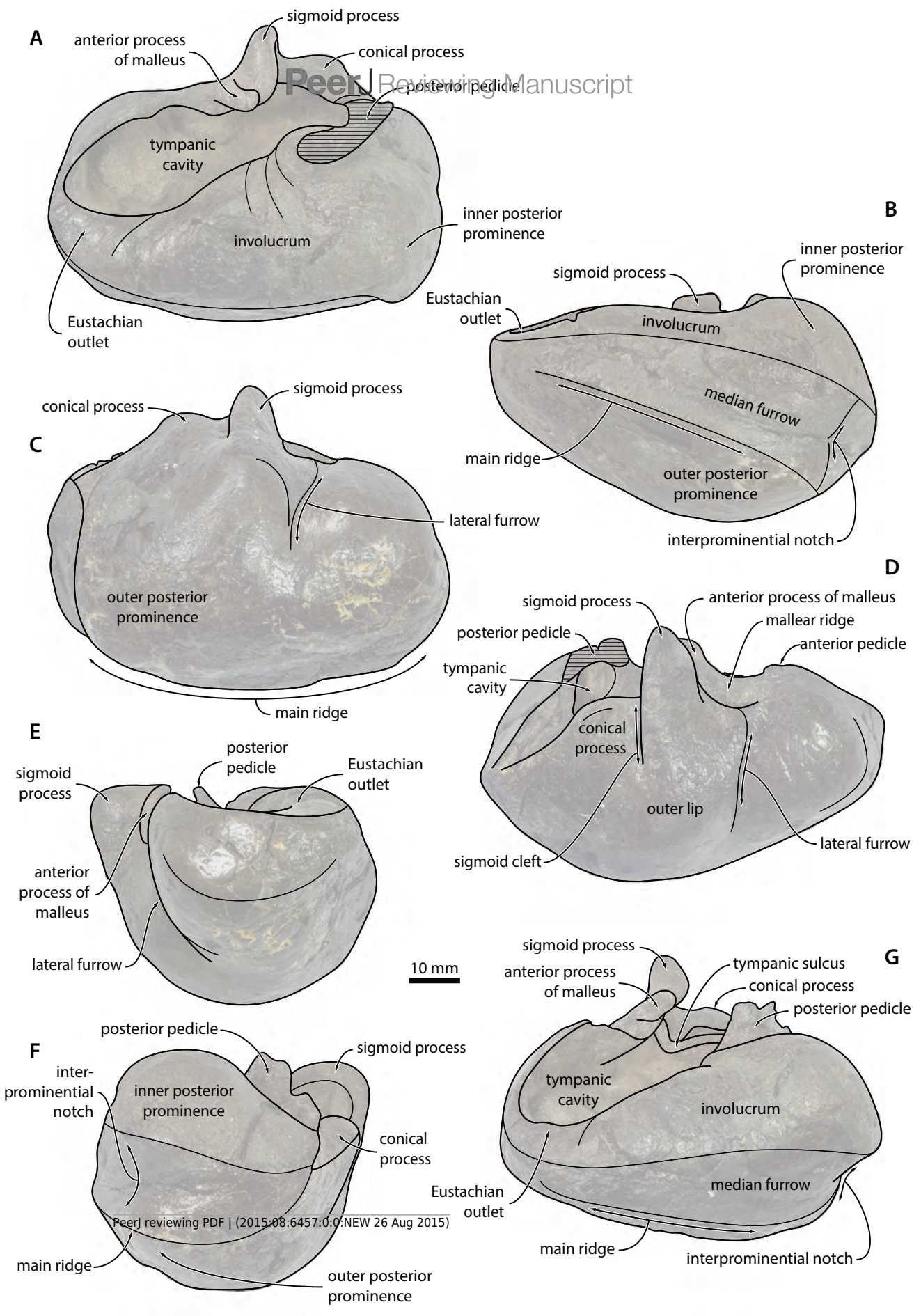

Figure 9(on next page)

Malleus

Figure 8. Malleus of *Metopocetus hunteri* in (a) posterior and (b) anterior view.

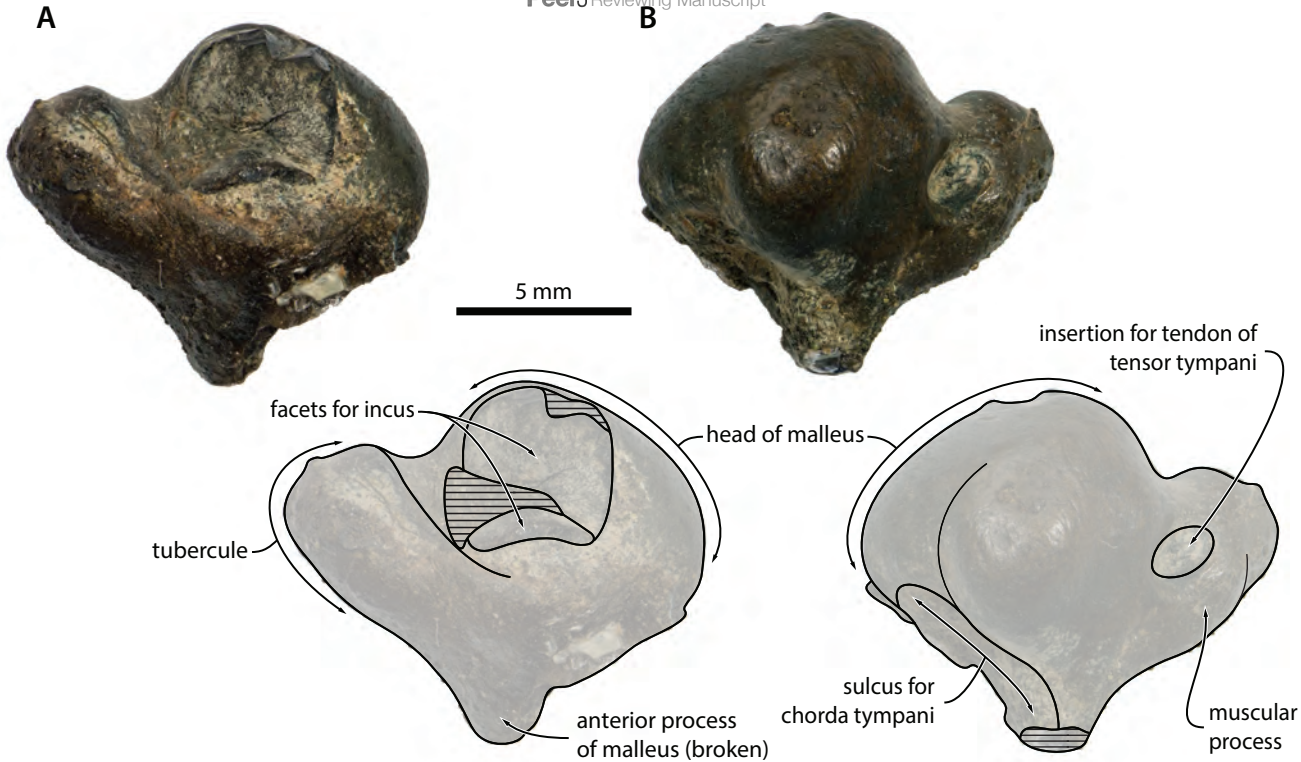
A
B
5 mm
facets for incus
head of malleus
tubercule
anterior process
of malleus (broken)
insertion for tendon of
tensor tympani
sulcus for
chorda tympani
muscular
process

Figure 10(on next page)

Phylogenetic relationships of Metopocetus hunteri

Figure 9. Phylogenetic relationships of *Metopocetus hunteri*, based on a dated total evidence analysis. All data except the codings for *M. hunteri* are from Marx & Fordyce (2015: fig. 2) . Drawings of cetaceans by Carl Buell.

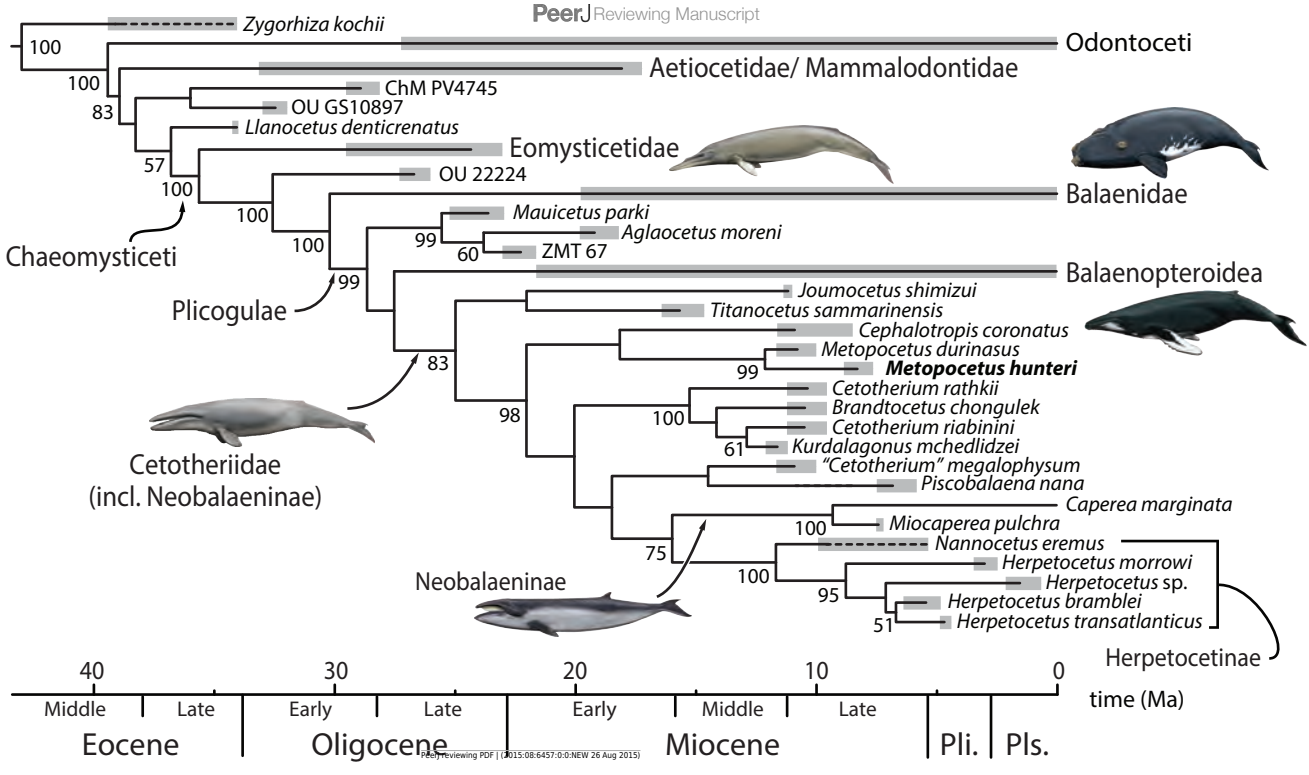
Zygorhiza kochii
Odontoceti
Aetiocetidae/ Mammalodontidae
ChM PV4745
OU GS10897
Llanocetus denticrenatus
Eomysticetidae
OU 22224
Balaenidae
Chaeomysticeti
Mauicetus parki
Aglaocetus moreni
ZMT 67
Balaenopteroidea
Plicogulae
Joumocetus shimizui
Titanocetus sammarinensis
Cephalotropis coronatus
Metopocetus durinasus
Metopocetus hunteri
Cetotheriidae
(incl. Neobalaeninae)
Cetotherium rathkii
Brandtocetus chongulek
Cetotherium riabinini
Kurdalagonus mchedlidzei
"Cetotherium" megalophysum
Piscobalaena nana
Caperea marginata
Miocaperea pulchra
Nannocetus eremus
Herpetocetus morrowi
Herpetocetus sp.
Herpetocetus bramblei
Herpetocetus transatlanticus
Neobalaeninae
Herpetocetinae
40
30
20
10
0
time (Ma)
Middle
Late
Early
Late
Early
Middle
Late
Eocene
Oligocene
Miocene
Pli.
Pls.

Figure 11(on next page)

Differences between *Metopocetus hunteri* and "*M.*" *vandelli*

Figure 10. Morphological features distinguishing "*Metopocetus*" *vandelli* from *M. durinasus* and *M. hunteri*. Skulls in dorsal view.

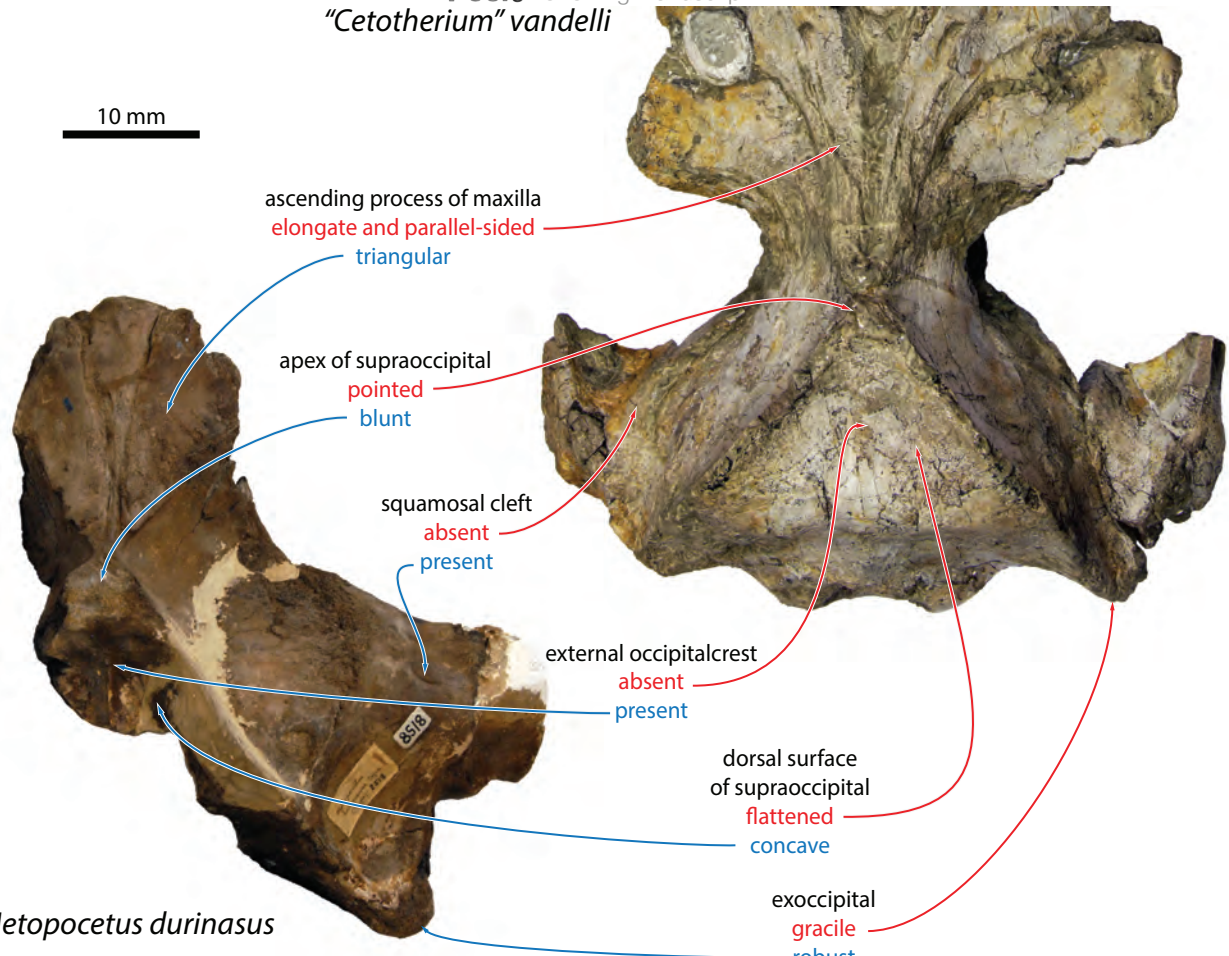
"Cetotherium" vandelli
10 mm
ascending process of maxilla
elongate and parallel-sided
triangular
apex of supraoccipital
pointed
blunt
squamosal cleft
absent
present
external occipitalcrest
absent
present
dorsal surface
of supraoccipital
flattened
concave
exoccipital
gracile
robust
8518
Metopocetus durinasus

Figure 12(on next page)

Basicranium of *Eschrichtius robustus*

Figure 11. Left portion of the basicranium of the extant grey whale, *Eschrichtius robustus*, in ventrolateral view, highlighting the position of the paroccipital concavity.

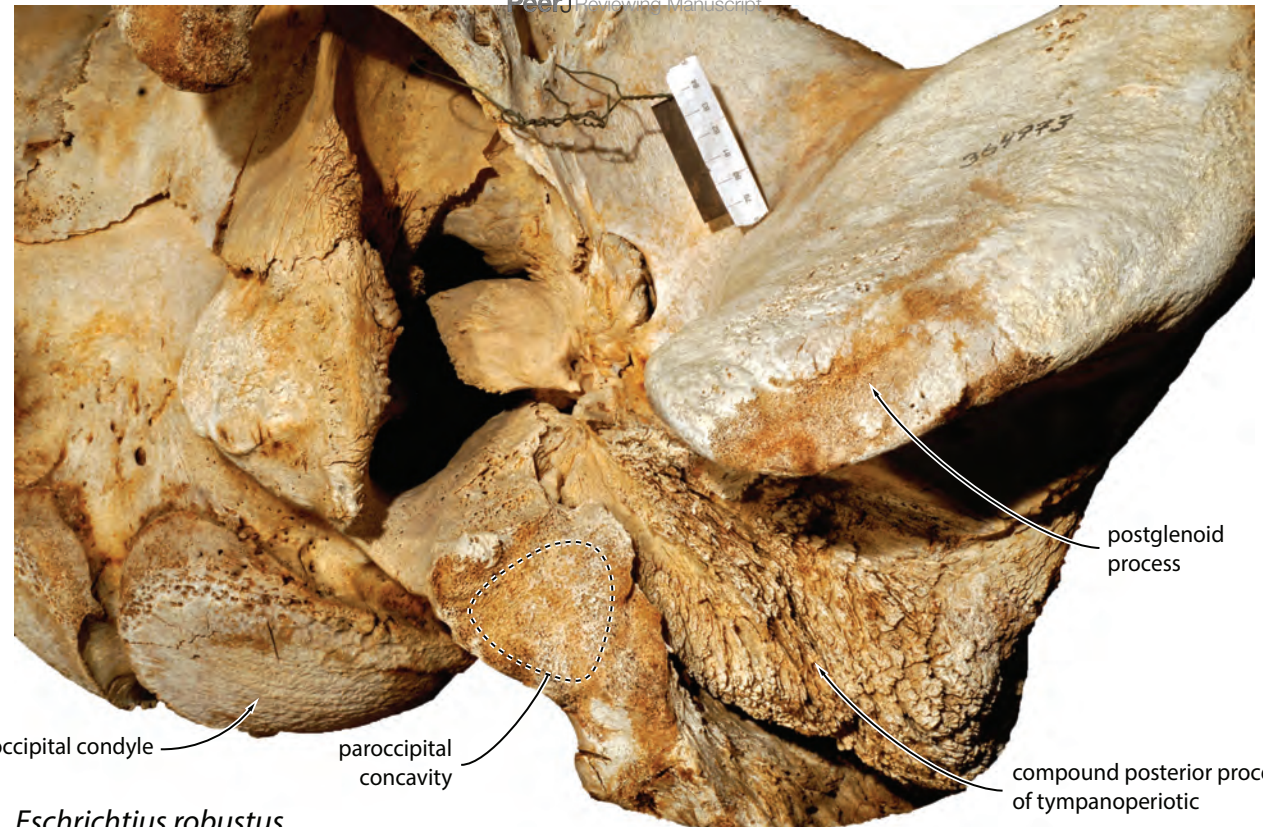

Eschrichtius robustus

Table 1(on next page)

Measurements of *Metopocetus hunteri*

Table 1 Measurements of *Metopocetus hunteri* (in mm).

1 **Table 1** Measurements of *Metopocetus hunteri* (in mm)

Maximum width of right occipital condyle	47.7
Bicondylar width*	150.0
Maximum distance between sagittal plane and outer surface of the zygomatic process, as preserved	285.0
Maximum distance between sagittal plane and lateral border of the exoccipital	190.0
Maximum length of right nasal, as preserved	137.0
Maximum length of left nasal, as preserved	155.0
Maximum anteroposterior diameter of paroccipital concavity	60.0
Maximum transverse diameter of paroccipital concavity	56.0
Maximum anteroposterior width of pars cochlearis, measured up to the medial border of the fenestra rotunda	18.6
Maximum anteroposterior length of tympanic bulla	77.1
Width of bulla just anterior to the sigmoid process	47.3
Maximum height of malleus, from the head to the tip of the tubercule	11.7

2 * estimated

3